15

Improvements of Hurricane Forecast with Vortex Initialization using WRF Variational (WRF-Var) Data Assimilation

Qingnong Xiao
College of Marine Science, University of South Florida
St. Petersburg, FL 33701,
USA

1. Introduction

Although the forecasts of hurricane track have steadily improved during the past two decades, intensity forecasts remain unsatisfactory (Elsberry, 2005). Previous studies have shown that vortex structures can significantly affect the behavior of hurricane intensity (Ross & Kurihara, 1995; Willoughby & Black, 1996; Xiao et al., 2000). The initialization of hurricane vortex as well as its environment using an advanced data assimilation technique is a key procedure to improve the accuracy of hurricane forecasts and to extend lead-time for hurricane forecasts with increased certainty. Particularly, assimilation of the data in the vortex region deserves more scientific research and technical development.

Assimilation of Doppler radar observations from coastal and aircraft Doppler radars in hurricane vortex initialization is of great interest to the weather service and research communities but with a lot of challenges (Liu et al., 1997; Marks et al., 1998; Xiao et al., 2000; 2006). The complexity comes from how we should establish the data assimilation system for hurricanes that are usually in the low latitude, compounded by a lack of data over the ocean and inadequate computer resources to resolve the inner core. From the several-year real-time hurricane forecasts using the Advanced-research Hurricane WRF (AHW) model (Davis et al., 2008; Xiao et al., 2009a; b), however, one conclusion is that an advanced analysis scheme has to be implemented for improved vortex initialization.

Data assimilation is a process that incorporates observations into numerical model with consideration of both observational data and model background information. There are several data assimilation techniques that can be used for hurricane initialization. The four-dimensional variational (4D-Var) data assimilation (Courtier et al., 1994) and Ensemble Kalman filters (EnKF, Evensen, 1994) are two of the most advanced in algorithm formulation and technique design. 4D-Var employs a forecast model as a strong constraint in a least-squares fit problem (Lewis & Derber, 1985, Le Dimet & Talagrant, 1986, Thepaut & Courtier, 1991, Navon et al., 1992). It has an implicit update of the flow-dependent background field and the capability to assimilate data at the exact observation time. The 4D-Var adjoint approach is an attractive assimilation technique. As a retrospective assimilation algorithm, it can derive the optimal time-trajectory fit to observational data, including non-synoptic data (Xiao et al., 2002, Simmons & Hollingsworth, 2002). 4D-Var has been

implemented for operational numerical weather prediction at many operational centers (e.g. ECMWF, Metero France, UK Met Office, & JMA). As we all know in the data assimilation community, however, the development of adjoint model is tedious, labor-intensive, and often subject to errors (Xiao et al., 2008a).

Another advanced data assimilation technique, EnKF, has gained much attention in recent years in the data assimilation community. EnKF can use flow-dependent background error covariance (**B** matrix) calculated from ensemble forecasts and can be easily implemented without tangent linear and adjoint models. Several formulations of EnKF have been developed, such as double EnKF (Houtekamer & Mitchell, 1998), ensemble square root filter (EnSRF, Whitaker & Hamill, 2001), ensemble adjust Kalman filter (EAKF, Anderson, 2001), ensemble transform Kalman filter (ETKF, Bishop et al., 2001), and local ensemble transform Kalman filter (Ott et al., 2004, Hunt et al., 2004). The advantages and weaknesses of 4D-Var and EnKF are discussed in Lorenc (2003), Gustafsson (2007) and Kalnay et al. (2007). The combination of advantages in 4D-Var and EnKF has attracted a lot of efforts in recent years (Evensen & van Leeuwen, 2000; Zupanski, 2005; Hunt et al., 2004; Fertig et al., 2007). Along this route, we proposed an ensemble-based four-dimensional variational (En4D-Var) algorithm (Liu et al., 2008; 2009). The new data assimilation technique, En4D-Var, uses the flow-dependent background error covariance matrix (**B** matrix) from the WRF ensemble, and performs 4D-Var optimization. It adopts the variational approach but avoids the tangent linear model and its adjoint, the component that is difficult to develop and that make 4D-Var minimization computationally expensive.

Since the establishment of the WRF-Var data assimilation system (Barker et al., 2004, Skamarock et al., 2005), we have contributed considerable efforts to develop the WRF adjoint (Xiao et al., 2008a), WRF 4D-Var (Huang et al., 2009), and WRF En4D-Var (Liu et al., 2009) under WRF-Var framework. However, most of the scientific researches, including hurricane initialization, still rely on the WRF 3D-Var system. During the past decade, remote sensing technology using Doppler radars has advanced rapidly to the point where synthetic dual Doppler observations are now available in real time from the extensive network of coastal radars and from reconnaissance aircraft. For example, Hurricane Rita (2005) was observed by the Key West WSR-88D (KBYX) while it was still a minimum hurricane. When Rita rapidly intensified in Gulf of Mexico into a Category 5 hurricane with a double eyewall, two NOAA P3s, NRL P3, Air Force C-130, and NOAA G-IV observed its structures in three consecutive days. During the TC08 campaign, the NRL P3 had several days of flight penetrating Typhoon Sinlaku. Obviously, hurricane initialization with these data can result in much better definition of the vortex structures.

Although storms approaching the coastline of North America and some typhoon cases in the western North Pacific are well sampled by both airborne and coastal radars, these data are currently being used primarily in the form of images for qualitative interpretation by forecasters. Several initialization techniques using Doppler radar data have been demonstrated to be effective. The mesoscale vorticity method (MVM, Lee et al., 2003, 2006) achieves improved initialization from high temporal resolution radar observations to compute the vertical velocity and radial flow from the better-observed rotational winds by Doppler radars. WRF 3D-Var can directly assimilate the Doppler radial winds and reflectivity data into analysis, which includes increments of vertical velocity and hydrometeors in the vortex initialization (Xiao et al., 2005; 2007; Xiao & Sun 2007; Xiao et al., 2008b). One of our recent efforts on hurricane vortex initialization has been shown that airborne Doppler radar (ADR) data assimilation can significantly enhance the hurricane

vortex (Xiao et al., 2009a). With the improved vortex, we are able to study the relationship of hurricane intensity change associated with its initial state and vortex structures, scale interaction between vortex and environment.

Hurricane intensity and intensity change are highly related to vortex structures. In order to have an accurate vortex structure in model forecasts, the initial conditions should be improved using observations in the vortex's inner core region. Numerical weather forecasting is an initial value problem. The enhanced analyses of vortex structure should provide sufficient detail and accuracy in support of the subsequent intensity forecasting. Unfortunately hurricanes are over oceans and there are usually no Doppler radar data available in the vortex region. Satellite data are not reliable due to cloud and precipitation contamination in the vortex. To define a hurricane structure in the model initial conditions, Xiao et al. (2000) and Zou & Xiao (2000) proposed the bogus data assimilation (BDA), a technique that assimilates a synthetic vortex using variational data assimilation to initialize the hurricane structure. With the optimization procedure, the synthetic vortex structures are gradually incorporated into the hurricane initial conditions. While BDA is initially applied to 4D-Var, it is now tested in 3D-Var systems (Xiao et al., 2006; 2009b). Computationally, BDA using 3D-Var is much faster than using 4D-Var. Because integrations of forward model and backward adjoint are involved in the iterative minimization procedure in 4D-Var, extensive experiments or real-time application of hurricane BDA with the 4D-Var framework have their difficulties. On the contrary, 3D-Var with BDA can be easily applied for large numbers of experiments. In addition, the WRF 3D-Var with BDA allows the hurricane structure to be generated by 3D-Var balance transform and background error covariance. Since the background error covariance is produced using WRF, the hurricane initialization can still achieve balance to some extent with the WRF model.

The BDA in WRF 3D-Var has been implemented based on the characteristics of WRF model (Skamarock et al., 2005). The preconditioned control variables are streamfunction, unbalanced velocity potential, unbalanced temperature, pseudo relative humidity, and unbalanced surface pressure. The NMC-method (Parrish & Derber, 1992) is used to construct correlations among the control variables for multivariate analysis. An asymmetric vortex perturbation is extracted from the previous forecast and relocated to the observed position. Summation of the symmetric vortex and the asymmetric perturbation produces a synthetic vortex structure. Assimilation of the synthetic sea-level pressure (SLP) and wind profiles are performed via the minimization procedure in the proposed BDA scheme in WRF 3D-Var. The radius of 34-kt wind in the hurricane advisory is used to calculate the bogus vortex size in BDA implementation (Xiao et al., 2006).

In the next section, a brief description of the WRF variational (WRF-Var) data assimilation technique is provided. The hurricane initialization experiments with Doppler radar data assimilation and BDA are discussed in Sections 3 and 4. In section 5 we summarize our work and draw some conclusions.

2. WRF Variational (WRF-Var) data assimilation

Hurricane initialization can be achieved through data assimilation approach, which blends observations with numerical model. Variational data assimilation achieves this through the iterative minimization of a prescribed cost (or penalty) function, so as to optimally synthesize observations in a model-consistent framework. Efforts have been made to perform vortex initialization for the Advanced-research Hurricane WRF (AHW, Davis et al.,

2008; Xiao et al., 2009b) using WRF-Var. The observations we used to better define the vortex structure are Doppler radar data and synthetic observations.

WRF-Var is a single software that combines 3 and 4-dimensional variational data assimilation systems for the WRF community. It includes WRF 3D-Var and WRF 4D-Var. The variational adjoint technique was introduced in 1980s (Lewis & Derber, 1985; Le Dimet & Talagrand, 1986), and it has played a more and more important role in numerical weather prediction (Daley, 1991; Rabier et al., 2000; Gustaffson, 2007; Kalnay et al., 2007; and Huang et al., 2009). Mathematically, variational data assimilation produces an optimal initial condition $\mathbf{x}_a$ by minimizing the cost function $J(\mathbf{x})$ in the assimilation window,

$$J(\mathbf{x}) = \frac{1}{2}(\mathbf{x}-\mathbf{x}_b)^T \mathbf{B}^{-1}(\mathbf{x}-\mathbf{x}_b) + \frac{1}{2}\sum_{i=0}^{I}(HM\mathbf{x}-\mathbf{y}_i)^T \mathrm{O}^{-1}(HM\mathbf{x}-\mathbf{y}_i). \quad (1)$$

In the equation, $\mathbf{x}_b$ is background state vector at t_0, H is observation operator, M is forecast model and $\mathbf{y}_i$ is observation vector at t_i, $\mathbf{B}$ is the background error covariance matrix and $\mathbf{O}$ is the observation error covariance matrix, and I is the total number of time levels at which observations are available. If all the observations are at one time and no forecast model is involved in the formulation, the problem is 3D-Var. If more than one-time observations are used and the model is involved in the formulation of (1), the problem becomes 4D-Var.

In the incremental approach (Courtier et al., 1994), the analysis increment $\mathbf{x}'$ instead of $\mathbf{x}$, is used in minimizing the cost function $J(\mathbf{x}')$ defined by

$$J(\mathbf{x}') = \frac{1}{2}(\mathbf{x}')^T \mathbf{B}^{-1}(\mathbf{x}') + \frac{1}{2}\sum_{i=0}^{I}(\mathbf{H}\mathrm{M}\mathbf{x}'+\mathbf{d}_i)^T \mathbf{O}^{-1}(\mathbf{H}\mathrm{M}\mathbf{x}'+\mathbf{d}_i), \quad (2)$$

where $\mathbf{x}' = \mathbf{x}-\mathbf{x}_b$ is the analysis increment vector, $\mathbf{H}$ is tangent linear observation operator, $\mathbf{M}$ is tangent linear forecast model, and $\mathbf{d}_i$ is the innovations at different time (with subscript i). $\mathbf{d}_i$ is calculated by

$$\mathbf{d}_i = HM(\mathbf{x}_b)-\mathbf{y}_i. \quad (3)$$

With the preconditioning (Gilbert et al., 1989) and introducing the preconditioning matrix $\mathbf{U}$ defined by

$$\mathbf{B} = \mathbf{U}\mathbf{U}^T, \quad (4)$$

we obtain the cost function in control variable ($\mathbf{w}$) space as,

$$J(\mathbf{w}) = \frac{1}{2}\mathbf{w}^T\mathbf{w} + \frac{1}{2}\sum_{i=0}^{I}(\mathbf{H}\mathrm{M}\mathbf{U}\mathbf{w}+\mathbf{d}_i)^T \mathbf{O}^{-1}(\mathbf{H}\mathrm{M}\mathbf{U}\mathbf{w}+\mathbf{d}_i). \quad (5)$$

The gradient of the cost function with respect to the control variables is

$$\nabla_{\mathbf{w}} J = \mathbf{w} + \sum_{i=0}^{I}\mathbf{U}^T\mathrm{M}^T\mathbf{H}^T\mathbf{O}^{-1}(\mathbf{H}\mathrm{M}\mathbf{U}\mathbf{w}+\mathbf{d}_i). \quad (6)$$

And the final analysis is

$$\mathbf{x}_a = \mathbf{x}_b + \mathbf{U}\mathbf{w} . \tag{7}$$

The WRF 3D-Var was developed from MM5 3D-Var (Barker et al., 2004), and has been adopted in real-time forecasting in several operational applications including Air Force Weather Agency (AFWA), Korean Meteorological Administration (KMA) and Taiwan Central Weather Bureau (CWB). It includes a background error covariance statistics package using either NMC method (Parrish & Derber, 1992) or ensemble method (Fisher, 1999). The cost function minimization is performed in terms of analysis increments. The analysis space is grid-point in the horizontal and a projection onto eigenvectors of the background error covariance matrix in the vertical. This projection allows efficient data compression at the expense of some spatial/temporal averaging of vertical error correlations. The WRF 4D-Var has recently developed based on the WRF model and 3D-Var as its basic components (Huang et al., 2009). It used the WRF 3D-Var framework that shares the same software engineering infrastructure as WRF. However, it possesses a number of advantages over 3D-Var including the ability to: a) use observations at the exact times that they are observed, which suits most asynoptic data; b) implicitly use flow-dependent background errors, which ensures the analysis quality for fast developing weather systems; and c) use a forecast model as a constraint, which enhances the dynamic balance of the final analysis. Almost all observations can be assimilated into WRF 3/4D-Var analysis, including the observations from GTS data stream, satellite (Liu & Barker, 2006) and Doppler radar (Xiao et al., 2005; 2007; Xiao & Sun 2007; Xiao et al., 2008b).

Recently, Liu et al. (2008; 2009) expanded WRF-Var to include the ensemble-based perturbation matrix in preconditioning. The advantage of WRF En4D-Var is that we can reformulate the algorithm to avoid tangent linear and adjoint models in calculating the gradient of cost function. However, the analysis is subject to the so-called sampling error problem in ensemble-based data assimilation. Liu et al. (2009) applied the Schur operator for localization in the WRF En4D-Var analysis and demonstrated that the localization technique can effectively alleviate the impacts of sampling errors upon analysis. The experimental results show that the WRF En4D-Var produced a better overall analysis than the WRF En3D-Var cycling. It suggests that the ensemble-based retrospective assimilation, WRF En4D-Var, has more robust analysis ability than ensemble-based sequential algorithms such as WRF En3D-Var cycling approach.

3. Hurricane initialization with Doppler radar data

3.1 Radial velocity

In order to include a capability to assimilate Doppler radial velocity data, the WRF 3D-Var was modified to include vertical velocity increments. Based on Richardson (1922) and White (2000), a balance equation that combines the continuity equation, adiabatic thermodynamic equation, and hydrostatic relation is derived and expressed as:

$$\gamma p \frac{\partial w}{\partial z} = -\gamma p \nabla \cdot \boldsymbol{V_h} - \boldsymbol{V_h} \cdot \nabla p + g \int_z^\infty \nabla \cdot (\rho \boldsymbol{V_h}) dz \tag{8}$$

where w is vertical velocity, $\boldsymbol{V_h}$ is the vector of horizontal velocity (components u and v), γ the ratio of specific heat capacities of air at constant pressure/volume, p pressure, ρ density, T temperature, c_p specific heat capacity of air at constant pressure, z height, and g the

acceleration due to gravity. For simplicity, hereafter Eq. (8) will be referred to as Richardson's equation. Linearizing Eq. (8) by writing each variable in terms of a basic state (overbar) plus a small increment (prime) gives

$$\begin{aligned}\gamma\bar{p}\frac{\partial w'}{\partial z} = &-\gamma p'\frac{\partial \bar{w}}{\partial z} - \gamma\bar{p}\nabla\cdot\boldsymbol{V_h'} - \gamma p'\,\nabla\cdot\overline{\boldsymbol{V_h}} - \overline{\boldsymbol{V_h}}\cdot\nabla p' \\ &-\boldsymbol{V_h'}\cdot\nabla\bar{p} + g\int_z^\infty \nabla\cdot(\bar{\rho}\boldsymbol{V_h'})dz + g\int_z^\infty \nabla\cdot(\rho'\overline{\boldsymbol{V_h}})dz\end{aligned} \quad . \tag{9}$$

The basic state (overbar) variables satisfy Eq. (8). They also satisfy the continuity equation, adiabatic equation and hydrostatic equation. The linear equation (9) is discretized, and its adjoint code is developed according to the code of the linearized equation (Xiao et al., 2005). The observation operator for Doppler radial velocity is

$$V_r = u\frac{x-x_i}{r_i} + v\frac{y-y_i}{r_i} + (w-v_T)\frac{z-z_i}{r_i}, \tag{10}$$

where (u,v,w) are the wind components, (x,y,z) are the radar location, (x_i,y_i,z_i) are the location of the radar observation, r_i is the distance between the radar and the observation, and v_T is terminal velocity. For radar scans at nonzero elevation angles, the fall speed of precipitation particles has to be taken into account. There are different ways to calculate terminal velocity. Here, we use the algorithm of Sun & Crook (1998) to calculate terminal velocity V_t (m/s),

$$v_T = 5.40a\cdot q_r^{0.125}, \tag{11}$$

where q_r is rainwater mixing ratio (g/kg). The quantity a is a correction factor defined by

$$a = (p_0/\bar{p})^{0.4}, \tag{12}$$

where $\bar{p}$ is the base-state pressure and p_0 is the pressure at the ground.

3.2 Reflectivity

Radar reflectivity measures the radar's signal reflected by precipitation hydrometeors. To assimilate radar reflectivity directly, the WRF 3D-Var system should be able to produce the increments of the hydrometeors (at least, the rainwater mixing ratio). We chose total water mixing ratio q_t as a control variable for reflectivity assimilation. Because total water mixing ratio q_t is used as a control variable, partitioning of the moisture and hydrometeor increments is necessary in the 3D-Var system (Xiao et al., 2007). We introduced the warm rain process of Dudhia (1989) for the partitioning, which includes condensation of water vapor into cloud (P_{CON}), accretion of cloud by rain (P_{RA}), automatic conversion of cloud to rain (P_{RC}), and evaporation of rain to water vapor (P_{RE}). These are the major processes of hydrometeor cycle in the summer season.

The tangent linear and its adjoint of the scheme were developed in the WRF 3D-Var system. Although the control variable is q_t, the q_v, q_c and q_r increments are produced through the partitioning procedure during the 3D-Var minimization. The warm rain scheme builds a constraint: the relation among rainwater, cloud water, moisture and temperature. When

rainwater information (from reflectivity) enters the minimization procedure, the forward warm rain process and its backward adjoint distribute this information to the increments of other variables (under the constraint of the warm rain scheme).
Once the 3D-Var system can produce q_c and q_r increments, the setup of the observation operator for assimilation of reflectivity is straightforward. We adopted the observation operator from Sun & Crook (1997):

$$Z = 43.1 + 17.5\log(\rho q_r), \tag{13}$$

where Z is reflectivity in the unit of dBZ and q_r is the rainwater mixing ratio. The relation (13) is derived analytically by assuming the Marshal-Palmer distribution of raindrop size.

3.3 Hurricane initialization with airborne Doppler radar data

We take Hurricane Jeanne (2004) as an example to illustrate the impact of the airborne Doppler radar (ADR) data assimilation on the vortex structure in the initial conditions as well as subsequent forecast. We conducted four sets of experiments: the control run CTL which uses the NCEP/GFS as the initial condition; the experiment GTS which assimilates only the conventional GTS data; GRV which assimilates GTS plus ADR wind data; and GVZ which is the same as GRV except both the ADR wind and reflectivity are assimilated.
Figure 1 shows the sea-level pressure (SLP) and 10-m winds with and without ADR wind assimilation for Hurricane Jeanne (2004) at 1800 UTC 24 September (the initialization time of the forecast). The cyclonic circulation is strengthened with a maximum surface wind (MSW) speed increase to 38 ms^{-1} (Fig. 1c), compared with 23.4 ms^{-1} in GTS (Fig. 1 b) and 23.7 ms^{-1} in CTL (Fig. 1a). The observed MSW speed is 44 ms^{-1}. Its CSLP is decreased in GRV after assimilating ADR wind data. Along with the intensity enhancement in wind speeds, the CSLP is correspondingly decreased about 5 hPa through the multivariate constraint in WRF 3D-Var. The GRV wind speed distribution in Figure 1c is much closer to the H*WIND (figure omitted) than those in Figures 1a and 1b.
WRF 3D-Var also produces temperature increments using ADR data due to the multivariate incremental structure in the system (Fig. 2). At 300 hPa, both temperature and wind vector increments in the vortex region in GTS are small (Fig. 2a), because no GTS observations exist in the vortex at high levels. The small increments for both the wind vector and temperature in the vortex region are due to the covariance with the environment. However, once assimilating the ADR winds in the vortex region, positive temperature increments occur associated with the strong wind vector increments and the maximum positive temperature increment is 1.117^{o}C at 300 hPa (Fig. 2b). In the cross-sections above the hurricane vortex, GTS shows only slight increments of temperature above 850 hPa (Fig. 2c). On the contrary, GRV produces a vertical incremental structure with the largest positive temperature increments in the high troposphere around 300 hPa. In the middle troposphere around 500 hPa, there is a negative layer of temperature increments. Notice that both GTS and GRV produce negative temperature increments above the vortex near the surface, due to the buoys and ships data assimilation. It is clear that the ADR data assimilation not only improves the 3-dimensional inner vortex wind structure, but also contributes to the vortex's warm core structure as well. The temperature response to the wind increments is rather small, due to the "climatological" error covariance from one-month forecasts as opposed to more flow-dependant error covariance that would know about the presence of the

hurricane. Vortex region is highly imbalanced; the "climatological" error covariance can only construct a small part of the warm core, a highly unbalanced structure.

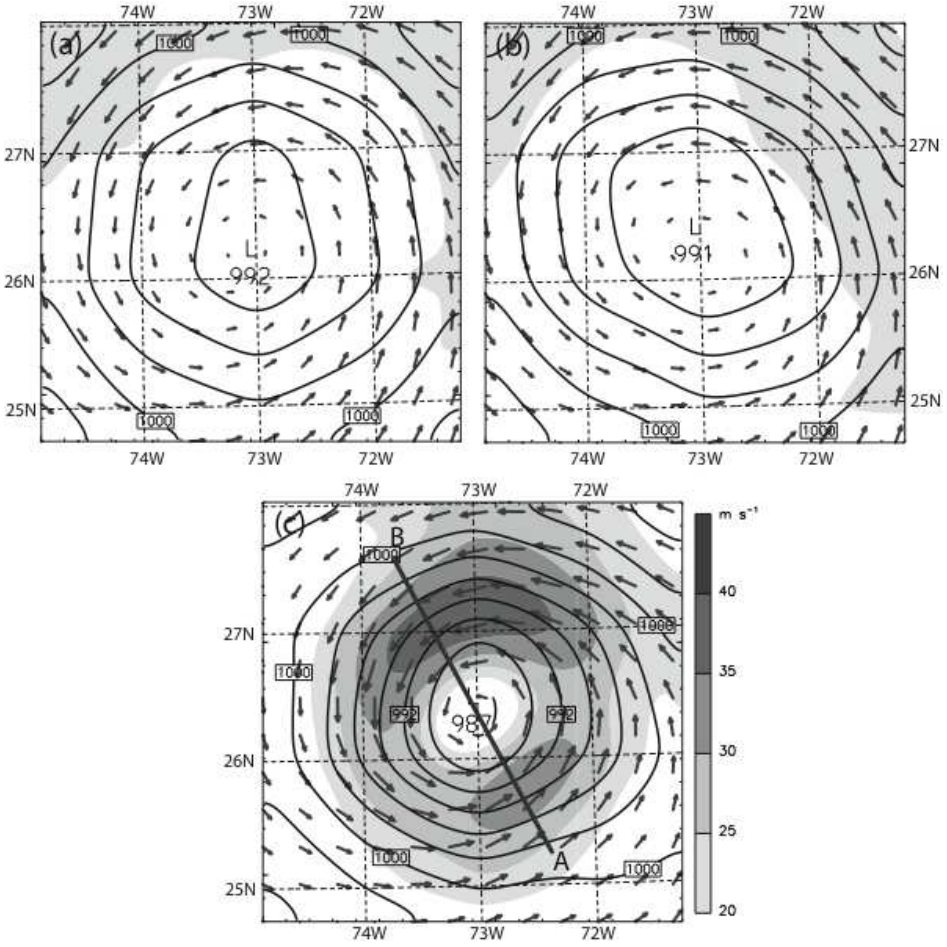

Fig. 1. SLP (thick solid isolines), and surface (10 m) wind vector and speed (shading with thin isolines) for Hurricane Jeanne at 1800 UTC 24 Sep 2004 by experiments (a) CTL, (b) GTS, and (c) GRV. The shading scale for surface wind speed is on the lower right.

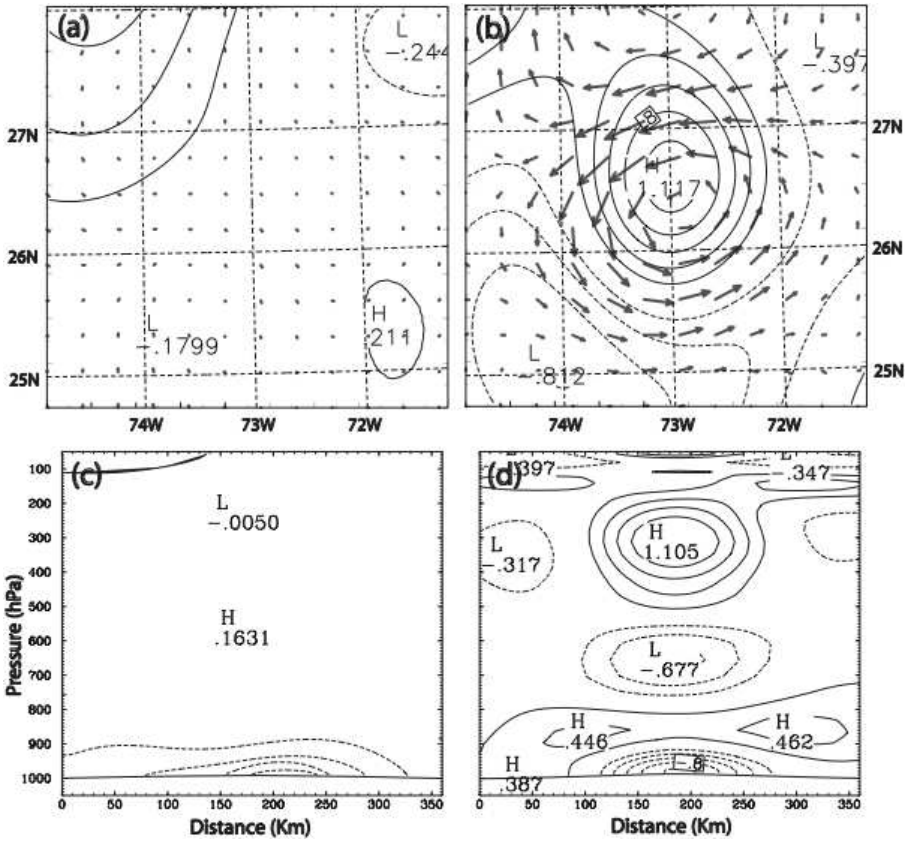

Fig. 2. 300-hPa analytical increments of wind vector (maximum vector represents 29.7 m s^{-1}) and the temperature (isolines with contour interval of 0.2 K, the negative value dashed) by experiments (a) GTS and (b) GRV, and cross sections of temperature increments (0.2 K interval) across the vortex from west to east in (c) GTS and (d) GRV.

Figure 3 shows the ADR reflectivity assimilation results of Hurricane Jeanne at 1800 UTC 24 September 2004 in the GVZ experiment. The CSLP (987 hPa) and 10-m wind analysis in GVZ (Fig. 3a) are similar to the results of GRV (Fig. 1c). However, GVZ produces cloud water and rainwater analyses after assimilating reflectivity data. Because the microphysics involved in the reflectivity assimilation has many "on-off" switches, the linearity assumption used in the WRF 3D-Var for the reflectivity assimilation is compromised. In addition, the warm-rain scheme in WRF 3D-Var does not represent well the microphysical process above the melting level (~ 500 hPa) for hurricanes. Nevertheless, GVZ contains some hydrometeor representation in the initialization, compared to no hydrometeors in GRV.

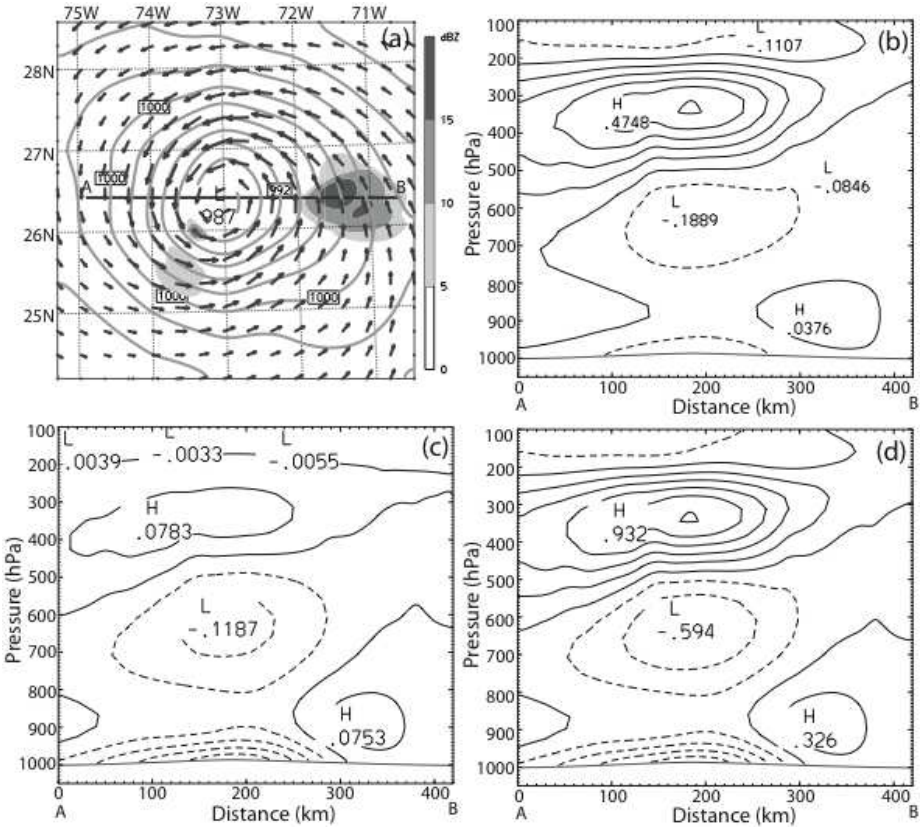

Fig. 3. Initialization with ADR reflectivity assimilation for Hurricane Jeanne at 1800 UTC 24 Sep 2004 by GVZ experiment: a) surface analysis of SLP (gray isolines with the interval of 2 hPa), 10-m wind (arrows with the maximum vector representing 38.4 ms^{-1}), and recovered composite reflectivity (dBZ) in the analysis (shading with the scales on the right), and cross-sections of b) temperature difference (with 0.1^{o}K interval), c) water vapor mixing ratio difference (with 0.05 g kg^{-1} interval), and d) equivalent potential temperature (q_e) difference (with 0.2^{o}K interval) between GVZ and GRV (GVZ-GRV) above the hurricane vortex along the line AB in a).

Figure 3b-d illustrates the changes occurring in variables not directly assimilated owing to the addition of reflectivity data. These changes arise from the multivariate structure in the analysis. The temperature and water vapor mixing ratio in the mid-to-lower levels above hurricane vortex are decreased, while in upper levels are increased (Figs. 3b and 3c). The storm center's stability $\frac{\partial \theta_e}{\partial z}$ increases (Fig. 3d), while at about 120 km radius, the stability between 900 and 500 hPa decreases, with a maximum difference of q_e at around 900 hPa. GVZ also produces a warmer upper level core. In general, ADR reflectivity assimilation increases the atmospheric stability in the vortex center, while decreasing stability outside the eye region. Figure 4 shows the composite reflectivity at 24- and 36-h forecasts for GTS, GRV and GVZ experiments. Experiment GTS does not produce an eye wall, indicating that the

vortex is not well organized (Fig. 4a & d). However, GRV and GVZ produce well-organized hurricane structures in reflectivity with compact eyewalls embedded in the vortex. Comparison of the observed reflectivity at landfall (figure omitted) with these forecasts suggests that both GRV and GVZ produce a realistic distribution of reflectivity, but the heavier rainband over the east coast of Florida and the suggestion of a break in reflectivity on the east side of the eye wall in GVZ matches the observations somewhat better.

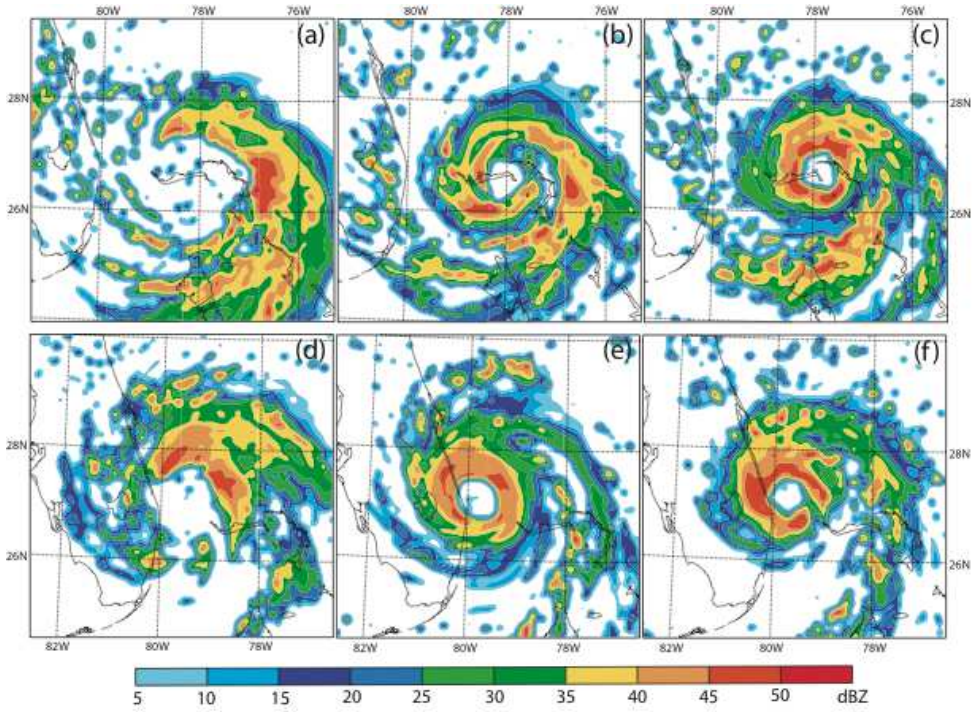

Fig. 4. The column maximum radar reflectivity (dBZ) at 1800 UTC 25 Sep (24-h forecast) for experiments a) GTS, b) GRV, and c) GVZ, and at 0600 UTC 26 September (36-h forecast) for experiments d) GTS, e) GRV, and f) GVZ.

We also carried out ADR data assimilation experiments for Hurricanes Katrina and Rita (2005). Verification of track and intensity for Hurricanes Jeanne (2004), Katrina and Rita (2005) indicates that ADR data assimilation improves the intensity forecast for all three hurricanes. The forecast improvement in track is not as significant as in intensity, but is noticeable. It is consistent with that the hurricane track mostly influenced by the environment, instead of the inner structure of hurricane. Hurricane intensity forecast is more significantly improved by ADR data assimilation than track. While GTS data shows no universal benefits for the intensity forecast, the CSLP average mean absolute errors with ADR data initialization are reduced at each forecast lead time within 48 h. The improvement in MSW is maintained for roughly 30 h, echoing the results for Jeanne alone. Significant reduction of MSW mean absolute errors occurs at the initial time. On average, the error reduction is nearly 29 (25) kt by the ADR data initialization in GRV (GVZ). In response to the vortex wind correction, the average decrease of CSLP from the three cases is about 7

hPa, which is not as significant as the MSW increase. The results indicate that the current correlation between CSLP and MSW is relatively weak in WRF 3D-Var system. The increments in vortex dynamical fields obtained by assimilating ADR wind do not result in a correspondingly large pressure response. Because the background error statistics used in this study were based on statistics averaged over an entire month, they are not flow-dependent and therefore do not reflect the vortex structure among variables in the background covariance. We anticipate further improvements by using specific error covariance that recognizes the hurricane vortex structure.
Nevertheless, the hurricane intensity forecasts are improved with ADR data assimilation using the relatively computationally inexpensive 3D-Var approach. The largest error reduction of CSLP and MSW occurs at 24 h. At 48 h, the CSLPs of both GRV and GVZ experiments still show less error than CTL and GTS.

4. Bogus data assimilation

To better define the vortex structure in hurricane initial conditions, a bogus data assimilation (BDA) scheme is developed in the WRF-Var. The BDA algorithm includes: a) bogus vortex construction and error specification, and b) assimilation of the bogus data with the WRF-Var system. In our studies (Xiao et al., 2006; 2009b; Zhang et al., 2007), the bogus vortex is constructed according to the method of Ueno (1989; 1995). There are two components (symmetric and asymmetric) in the bogus observations. The asymmetric component comes from 3D-Var background (previous forecast).
The bogus vortex fields include SLP and wind profiles at various levels. The distribution of SLP within the bogus area is calculated by the following equation based on the Fujita (1952) formula,

$$P(r) = P_{\max} - \frac{\Delta P}{\left(1 + \frac{1}{2}\left(\frac{r}{R_0}\right)^2\right)^{1/2}}, \tag{14}$$

where

$$\Delta P = P_{\max} - P_C, \tag{15}$$

$$P_{\max} = P_C + \frac{P_B - P_C}{1 - \frac{1}{1 + (R_B / R_0)^2}}. \tag{16}$$

In the equations of (14)-(16), r is the distance from the hurricane center (km), R_0 is the radius of maximum wind, P_C is the reported central SLP, and P_B is the average SLP within R_B. R_B is a predefined radius of the bogus area.
The bogus symmetric wind is based on the gradient wind relation,

$$V(r) = \left(\frac{r}{\rho}\frac{\partial P}{\partial r} + \frac{f^2 r^2}{4}\right)^{1/2} - \frac{r|f|}{2}. \tag{17}$$

Empirically, we include the effect of surface friction near the boundary layer by specifying smaller weightings. There are 7 levels (sea-level, 1000, 925, 850, 700, 600, 500 hPa) in the

bogus wind profile. The weightings of the symmetric wind speed for each layer are 0.7, 0.8, 0.9, 1.0, 1.0, 1.0, 1.0, respectively. The divergence of upper air is difficult to determine. Therefore, the bogus symmetric winds are assigned 0 in the upper levels above 400 hPa.

The asymmetric component is extracted from the WRF-Var background fields. When the background fields come from the WRF forecast, the position of the hurricane in the background fields can be different from observation. The asymmetric component is the difference between the background and the background typhoon symmetric component. Such asymmetric components are relocated to the right position and added to the symmetric bogus fields.

The bogus observation error is empirically specified. We assume that the error is linearly increased with respect to the distance from the typhoon center. Empirically, the specified errors of the bogus SLP and wind profiles are specified as follows:

$$E_{SLP}(r) = 1 + \frac{3}{R_B} r \,, \tag{18}$$

$$E_V(r,z) = E_{V0}(z) + \frac{4}{R_B} r \,, \tag{19}$$

where r is the distance from the hurricane center, z is the height, and R_B is the calculated radius of the bogus area. The errors of the bogus SLP range from 1 hPa in the center to 4 hPa around the outmost edge of the bogus area, compared to the constant surface observation error (2 hPa) for SYNOP. $E_{V0}(z)$ represents the errors of the bogus wind at the center. Its values range from 1 m/s at the sea level to 3.3 m/s at 250 hPa, the same as the other wind errors (e.g. TEMP, SATOB, PILOT, etc.). The specified errors of the bogus wind at sea level range from 1 m/s in the center to 5 m/s around the outmost edge of the bogus area.

The observation error specification is crucial in defining how the observation is used in a data assimilation system (Hollingsworth & Lonnberg, 1986). It determines how much of the observation is contributed to the analysis. However, the true values of the vortex bogus observation error are difficult to establish. The smaller error specified near the hurricane center implies more contribution from the bogus data near the center in the analysis. At the outmost edge of the bogus area, the bogus data have the smallest contribution. This also ensures a smooth transition of the analysis between the bogus area and the surrounding environment.

In the BDA, the hurricane bogus fields are treated as supplemental observations and are assimilated during the WRF-Var analysis. The cost function in Eq. (1) includes the contributions of the bogus data in the observation term. The observational operators for the SLP and wind profiles in the WRF-Var system are just an interpolation scheme because SLP and winds are direct variable of the model.

To verify the capability of BDA, we selected twenty-one cases from seven hurricanes in the 2004 and 2005 seasons to conduct parallel experiments. They are Hurricanes Charley, Frances, Ivan, and Jeanne in 2004, and Katrina, Rita, and Wilma in 2005. We selected three cases for each hurricane before its landfall. These cases are very famous due to their striking effects to Florida in 2004 and devastating impacts in the Gulf of Mexico in 2005. Two parallel sets of experiments are carried out. The first set of experiments (CT) for all cases use GFS (Global Forecast System) analysis as background and assimilate only the conventional GTS. The second set of experiments (GB) is the same as CT but including BDA. The WRF 3D-Var

experiments use the same background error covariance calculated from one-month statistics in September 2004 using the NMC method (Parish & Derber, 1992).

Figure 5 shows the mean absolute errors of the forecasts (position, CSLP, and MSW) against the best track observations at 24, 48, and 72 hours. The errors from the BDA experiments (GB) are smaller than that from control experiments (CT) for all of the verification parameters (position, CSLP, and MSW). Bogus data is able to remedy the data sparse issue in the vortex region and BDA improves the hurricane forecasting skill. We calculated the error reduction percentage by BDA from the statistics in Figure 5. The largest reduction of average error is in the forecast of CSLP, with 26.4% reduction of average error by BDA. The improvement in hurricane MSW is also significant; the average error is reduced by 24.0%. The track has the smallest but evident improvement among the three verification parameters.

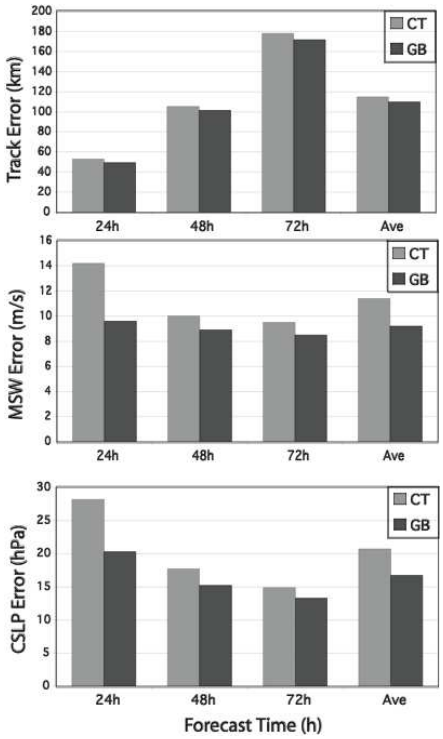

Fig. 5. The mean absolute errors of the hurricane track (top), MSW (middle) and CSLP (bottom) for the forecasts from statistics of 21 cases in 2004 and 2005.

Due to model spin-up problem, both sets of experiments (CT and GB) present smaller CSLP and MSW errors at 48 and 72 hours than at 24 hour. However, the spin-up problem in GB is much less than in CT. BDA alleviates the spin-up problem, and produces larger hurricane intensity improvement at 24 hour than at 48 and 74 hours. The benefit of BDA in hurricane intensity forecasts becomes less with the increase of the forecast time (Fig. 5). The initial intensity using BDA in GB experiments is much closer to the observed than CT. With the model runs, the difference of intensity between GB and CT decreases, reflecting the model forecast at longer time is less sensitive to initial conditions than at shorter time. The

improvement of hurricane CSLP and MSW in GB compared to CT at 24 hours is much more remarkable than that at 48 and 72 hours. In the track forecasts, however, experiment GB has the most significant improvement at 72 hours over the experiment CT.

Statistically, the improvement of hurricane intensity using BDA is more significant than that of hurricane track. It is further verified that the large-scale environment influences hurricane track, but that intensity is mainly impacted by hurricane's internal, dynamical and thermo-dynamical vortex structures. The BDA technique, which mainly improves the hurricane vortex structure according to the hurricane concept model, results in significant improvement of the hurricane intensity forecast. To support the assertion, we take Hurricane Katrina at 0000 UTC 26 August 2005 as an example to compare the vortex structures in CT and GB (Fig. 6). The CSLP and MSW errors are both reduced by BDA for Katrina initialized at 0000 UTC 26 August 2005. As shown in Figure 6, the hurricane positions of CT and GB are both very close to the observation. However, GB produces a vortex with lower CSLP and larger MSW than CT. BDA enhances the cyclone circulation and make the vortex much more compact. The area of the circular isobar with 1010hPa in GB is much reduced compared with that in CT. Note that the GFS analysis has its bogussing/relocation procedure, but it is apparently not sufficient for a good hurricane intensity forecast in the WRF ARW model. We verified that the initialization with BDA could improve the hurricane intensity forecast compared with the forecast from a simple GFS analysis.

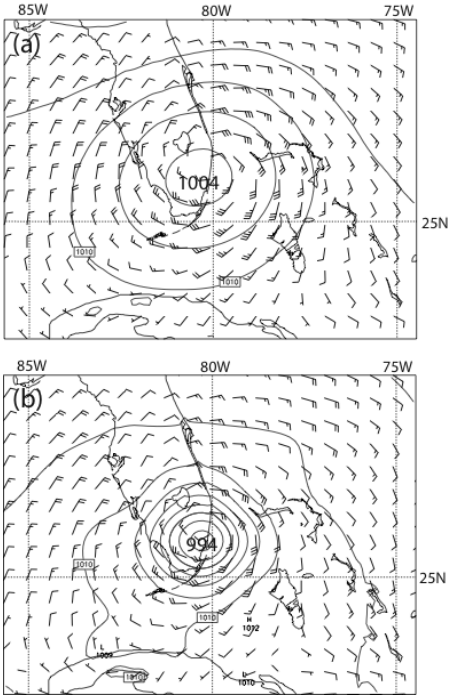

Fig. 6. Hurricane Katrina at 0000 UTC 26 August 2005. The solid lines are SLP (with interval of 2.5 hPa and the barbs show 10-m wind field (a full barb represents 5 m/s) for (a) CT and (b) GB experiments.

The GFDL bogus scheme (Kurihara et al., 1993) has been applied in hurricane initialization for over a decade. To further evaluate the performance of the BDA scheme in WRF 3D-Var, two parallel experiments on Hurricane Humberto at 1200 UTC 12 September 2007 are compared. The first experiment (CT) uses the WRF preprocessing system (WPS) to interpolate the GFDL analysis as initial conditions; and the second experiment (GB) uses the WRF 3D-Var procedure to initialize the hurricane vortex. The experiment GB uses GFS analysis as the first guess in WRF 3D-Var and assimilates the bogussing vortex plus conventional data. The forecasts for both experiments (CT and GB) are executed on 3 domains with the moving nested domains 2 and 3. The grid-spacings of the three domains are 12, 4, and 1.333 km, respectively.

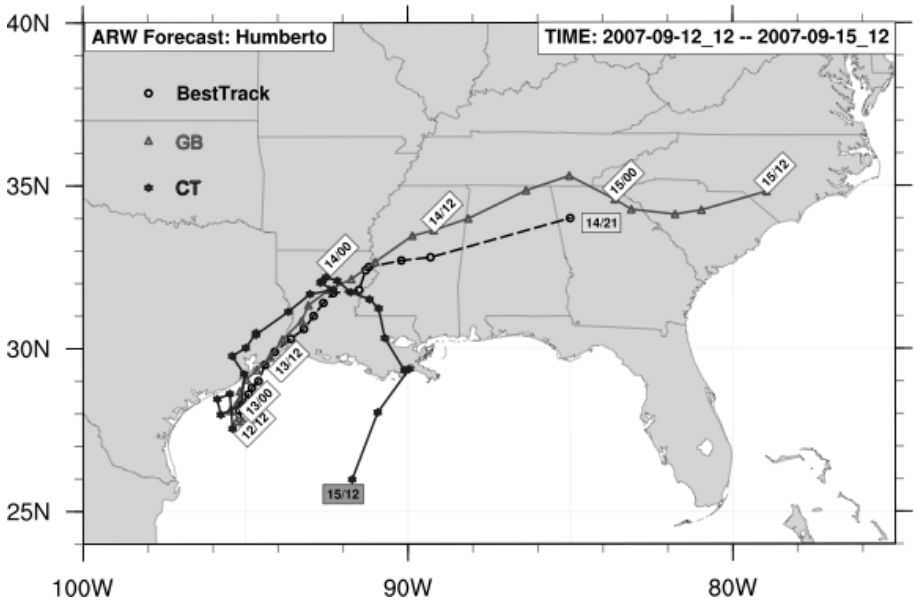

Fig. 7. 72-h track forecast for Hurricane Humberto starting from 1200 UTC 12 to 1200 UTC 15 September 2007. Dashed line with "o" is the best track; the solid line with "∗" is the forecast from CT experiment; and the grey line with "Δ" is the forecast from GB experiment. The date/hour are shown in boxes.

Figure 7 shows the forecasted tracks from experiments CT and GB as well as the best track for the period of 1200 UTC 12 - 1200 UTC 15 September 2007. The experiment CT, which has the vortex not well organized at the initial time, fails predicting the storm's inland movement. It lingers along the coastal area of Texas and Louisiana for two days, and then turns back to the Gulf of Mexico. Compared with the best track observation, CT fails to predict the storm's track. On the contrary, the experiment GB successfully predicts the storm's landfall and inland movement. Its predicted track follows the best track observation. Note that in Figure 7 the best track from the National Hurricane Center extends to 2100 UTC 14 September, while the prediction extends to 1200 UTC 15 September.

For the intensity prediction, CT also fails to predict the storm's intensification before landfall. Since it fails to predict the storms' intensification before landfall and fails to predict

the storm's inland movement, its overall intensity forecast is not successful at all and therefore omitted in the comparison. In Figure 8, we thus only analyze the storm's intensity in GB and compare it with observation. The trends of CSLP (Fig. 8a) and MSW (Fig. 8b) from 1200 UTC 12 to 1200 UTC 15 September show good agreement between the forecast and observation. GB successfully predicts Humberto's intensification from a tropical storm (1200 UTC 12 September) to a Category-1 hurricane (0600 UTC 13 September) before its landfall over the Texas coast. The observation indicates the maximum intensity of Humberto at 0915 UTC 13 September with a CSLP of 986 hPa and a MSW of 85 kt (44 m/s). GB predicts the maximum intensity at 0945 UTC 13 September with a CSLP of 989 hPa and a MSW of 82 kt (43 m/s). However, it over-predicts Humberto's strength inland. At 0000 UTC 14 September, for example, GB predicts a CSLP of 997 hPa and a MSW of 37 kt (19 m/s), while the observations are 1006 hPa and 25 kt (13 m/s).

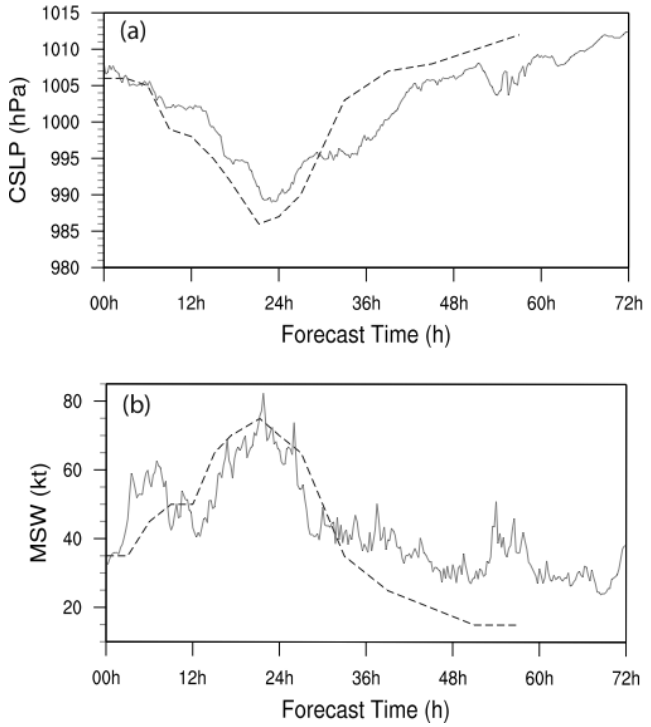

Fig. 8. 72-h intensity forecast for Hurricane Humberto starting from 1200 UTC 12 to 1200 UTC 15 September 2007: (a) Central sea level pressure (CSLP), and (b) Maximum surface wind (MSW). The solid line is the forecast from the GB experiment and dashed line is from the best track observation.

5. Summary and conclusions

Hurricane initialization using the data in the vortex region is important for the intensity forecast. Doppler radar data and synthetic bogus data assimilations (BDA) have been implemented in WRF variational data assimilation (WRF-Var) system, and positive impacts

on the analysis and forecast of hurricane structure and intensity have been obtained (Xiao et al., 2009a; b). The capability of airborne Doppler radar (ADR) data assimilation to improve hurricane initialization using WRF 3D-Var is examined for Hurricanes Jeanne (2004), Katrina (2005), and Rita (2005). The BDA technique is tested using 21 cases from 7 hurricanes in the 2004 and 2005 seasons. We also conducted one case study for Hurricane Humberto (2007), and compared the results between BDA and GFDL analyses for the WRF runs. The followings are highlights of our findings from the experiments:

- Assimilation of Doppler radial wind data markedly improve the representation of the hurricane vortex structure both at the initial time and in the forecast out to about 36 h. The ADR wind assimilation makes important contributions to improving hurricane intensity and structure forecasts. Hurricane track forecasts also benefited from assimilation of ADR wind data.
- The ADR reflectivity data assimilation in WRF 3D-Var system retrieves portion of the three-dimensional rainwater and cloud water fields of hurricane vortex at initialization. The multivariate responses in other variables are also reasonable. The addition of ADR data produces a realistic eye wall and associated strong convection. Rain bands are also favorably reorganized and appear more realistic.
- WRF hurricane forecasting using the BDA technique shows an improved forecast skill in hurricane track and intensity compared to initialization from just GFS analysis. Using the WRF 3D-Var system, the bogus SLP and wind profile data can be efficiently assimilated to recover the initial hurricane structure under 3D-Var statistical and physical balances. The forecasts of hurricane track and intensity are therefore improved.
- The enhancement of the hurricane forecast skill using BDA technique reflects in all forecast periods. With BDA, the largest improvement is in hurricane central pressure. The improvement in hurricane maximum surface wind is also statistically significant. The track has the smallest improvement among the three verification parameters.
- BDA with WRF 3D-Var performs well in a case study of Hurricane Humberto (2007), whereas WRF with the initial conditions interpolated from the GFDL analysis failed in the hurricane's landfall. More cases studies and real-time forecasts are necessary to further verify its performance. However, BDA with WRF 3D-Var for hurricane initialization has the potential to improve WRF hurricane forecasts.

One of the most challenges for the hurricane forecaster and researcher is to define the vortex structure in light of insufficient observations over the ocean. The Doppler radar data (from coastal radar or airborne Doppler radar) are valuable data source for hurricane structure. When there is no data at all in the vortex region, synthetic bogus data would help in defining the vortex structure. The BDA has shown promise in WRF hurricane forecasts. Usually, satellite data are less useful within the vortex due to cloud and rainfall contamination, limited spatial resolution, or suboptimal timing of observations (from polar orbiting platforms, for instance). Assimilating Doppler radar data or sometimes synthetic bogus vortex data is feasible and should be considered in forecasting of landfalling hurricanes so as to reduce the loss of life and property in coastal regions.

In terms of WRF 3D-Var for hurricane vortex initialization, some limitations also exist. Firstly, a specific background error covariance for hurricanes should be developed and used in hurricane initialization. The background error statistics used in our studies are from the traditional NMC technique (Parrish & Derber, 1992). It is not totally suitable for the correlations in the hurricane vortex. The correlation of wind and pressure only presents

large-scale feature. Secondly, reflectivity assimilation in WRF 3D-Var uses warm-rain process to bridge rainwater with other model variables in the analysis. At high levels above melting layer, however, ice-phase hydrometeors contribute to the most of reflectivity measurement. In this regard, a sophisticated microphysics that builds relationships among the whole hydrometeors and other dynamical and thermo-dynamical variables should be developed in WRF 3D-Var for radar reflectivity data assimilation. Finally, observation error statistics for radar observations and bogus data are only crudely represented at present. In addition, it should also be noted that most of our studies are based on the WRF 3D-Var that does not take into account the time differences but instead ingests data at one instant in time. 4D-Var should be a future direction for hurricane vortex initialization in order to better initialize the time dependence of the vortex necessary to accurately capture rapid intensity change as it is occurring.

6. References

Anderson, J. L. (2001). An ensemble adjustment Kalman filter for data assimilation. *Mon. Wea. Rev.*, **129**, 2884–2903.

Barker, D. M.; Huang, W.; Guo, Y.-R.; Bourgeois, A. J. & Xiao, Q. (2004). A three-dimensional (3DVAR) variational data assimilation system for MM5: implementation and initial results. *Mon. Wea. Rev.*, 132, 897-914.

Bishop, C.H.; Etherton, B.J. & Majumdar, J. S. (2001). Adaptive Sampling with the Ensemble Transform Kalman Filter. Part I: Theoretical Aspects. *Mon. Wea. Rev.*, 129, 420-436.

Courtier, P.; Thepaut, J.-N. & Hollingsworth, A. (1994). A strategy for operational implementation of 4D-Var using an incremental approach. *Quart. J. Roy. Meteor. Soc.*, 120, 1367–1387.

Daley, R. (1991). *Atmospheric data analysis*, Cambridge University Press. Cambridge UK.

Davis, C. A.; Wang, W.; Chen, S. S.; Chen, Y.; Corbosiero, K.; DeMaria, M.; Dudhia, J.; Holland, G. J.; Klemp, J.; Michalakes, J.; Reeves, H.; Rotunno, R. & Xiao, Q. (2008). Prediction of landfalling hurricanes with the advanced hurricane WRF model. *Mon. Wea. Rev.*, 136, 1990-2005..

Dudhia, J. (1989). Numerical study of convection observed during the winter monsoon experiment using a mesoscale two-dimensional model. *J. Atmos. Sci.*, 46, 3077-3107.

Elsberry, R. L. (2005). Achievement of USWRP hurricane landfall research goal. *Bull. Amer. Meteor. Soc,* 86, 643-645.

Evensen, G. (1994). Sequential data assimilation with a nonlinear quasi-geostrophic model using Montre Carlo methods to forecast error statistics. *J. Geophys. Res.,* 99, 10, 143-10,162.

Evensen, G. & van Leeuwen, P. J. (2000). An ensemble Kalman smoother for nonlinear dynamics. *Mon. Wea. Rev.,* 128, 1852–1867.

Fertig, E. J.; Harlim, J.; & Hunt, B. R. (2007). A comparative study of 4D-VAR and a 4D Ensemble Filter: perfect model simulations with Lorenz-96. *Tellus*, 59A, 96-100.

Fisher, M. (1999). Background error statistics derived from an ensemble of analyses. *ECMWF Research Department Tech. Memo.*, 79, 12pp.

Gustafsson, N. (2007). Discussion on "4D-Var or EnKF?", *Tellus,* 59A, 774-777.

Hollingsworth, A. & Lo¨nnberg, P. (1986). The statistical structure of short-range forecast errors as determined from radiosonde data. Part I: The wind field. *Tellus*, 38A, 111–136.

Houtekamer, P. L. & Mitchell, H. L. (2001). A Sequential Ensemble Kalman Filter for Atmospheric Data Assimilation. *Mon. Wea. Rev.,* 129, 123-137.

Huang, X.-Y.; Xiao, Q.; Barker, D. M.; Zhang, Xin; Michalakes, J.; Huang, W.; Hendersen, T.; Bray, J.; Chen, Y.-S.; Ma, Z.; Dudhia, J.; Guo, Y.-R.; Zhang, X.; Won, D.-J.; Lin, H.-C. & Kuo, Y.-H. (2008). Four-dimensional variational data assimilation for WRF: Formulation and preliminary results. *Mon. Wea. Rev*., 137, 299-314.

Hunt, B. R.; Kalnay, E.; Kostelich, E. J.; Ott, E.; Patil, D. J.; Sauer, T.; Szunyogh, I.; Yorke, J. A. & Zimin, A. V. (2004). Four-dimensional ensemble Kalman filtering. *Tellus*, 56A, 273-277.

Kalnay, E.,; Li, H.; Miyoshi, T.; Yang, S.-C. & Ballabrera-Poy, J. (2007). 4D-Var or Ensemble Kalman filter? *Tellus*, 59A, 758-773.

Kessler, E. (1969). *On the Distribution and Continuity of Water Substance in Atmospheric Circulation*. *Meteor. Monogr.,* 32, Amer. Meteor. Soc., 84 pp.

Kurihara, Y.; Bender, M. A. & Ross, R. J. (1993). An initialization scheme of hurricane models by vortex specification. *Mon. Wea. Rev*., 121, 2030–2045.

Le Dimet, F.-X. & Talagrand, O. (1986). Variational algorithms for analysis and assimilation of meteorological observations: Theoretical aspects, *Tellus*, 38A, 97-110.

Lee, J.-L.; Kuo, Y.-H. & MacDonald, A. E. (2003). The vorticity method: Extension to mesoscale vertical velocity abd validation for tropical storms. *Quart. J. Roy. Meteor., Soc*., 129, 1029-1050.

Lee, J.-L.; Lee, W.-C. & MacDonald, A. E. (2006). Estimating vertical velocity and radial flow from Doppler radar observations of tropical cyclones. *Quart. J. Roy. Meteor. Soc*., 132, 125-145.

Lewis, J. M. & Derber, J. C. (1985). The use of adjoint equations to solve a variational adjustment problem with advective constraints. *Tellus,* 37A, 309–322.

Liu, C.; Xiao, Q. & Wang, B. (2008). An ensmble-based four-dimensonal variational data assimilation scheme. Part I: technical formulation and preliminary test. *Mon. Wea. Rev*., 136, 3363-3373.

Liu, C.; Xiao, Q. & Wang, B. (2009). An ensemble-based four-dimensional variational data assimilation scheme. Part II: Observing syetem simulation experiments with advanced research WRF (ARW). *Mon. Wea. Rev*., 137, 1687-1704..

Liu, Y.; Zhang, D.-L. & Yau, M. K. (1997). A multiscale numerical study of Hurricane Andrew (1992). Pat I: Explicit simulation and veridication. *Mon. Wea. Rev*., 125, 3073-3093.

Liu, Z. & Barker, D. M. (2006). Radiance assimilation in WRF-Var: Implementation and initial results. *Preprint of the 7th WRF user's workshop*, Boulder, Colorado, 19-22 June 2006.

Lorenc, A. (2003). The potential of the Ensemble Kalman Filter for NWP: a comparison with 4DVar. *Quart. J. Roy. Meteor. Soc*., 129, 3183–3203.

Marks, F. D.; Shay, L. K.; Barnes, G.; Black, P.; DeMaria, M.; McCaul, B. & Molinari, J. (1998). Landfallinhg tropical cyclones: forecast problems and associated research opportunities. *Bull. Amer. Met. Soc*., 79, 305-323.

Navon, I. M.; Zou, X.; Derber, J. & Sela, J. (1992). Variational Data Assimilation with an Adiabatic Version of the NMC Spectral Model. *Mon. Wea. Rev.*, 120, 1381–1393.

Ott, E; Hunt, B. R.; Szunyogh, I. ; Zimin, A. V. ; Kostelich, E. J. ; Corazza, M.; Kalnay, E.; Patil, D. J. & Yorke, J. A. (2004). A local ensemble Kalman filter for atmospheric data assimilation. *Tellus*, 56A, 415-528.

Parrish, D. F. & Derber, J. C. (1992). The National Meteorological Center's Spectral Statistical Interpolation analysis system. *Mon. Wea. Rev.,* 120, 1747–1763.

Rabier, F.; Jarvinen, H.; Klinker, E.; Mahfouf, J.-F. & Simmons, A. (2000). The ECMWF operational implementation of four-dimensional variational assimilation. Part I: Experimental results with simplified physics. *Quart. J. Roy. Meteor. Soc.*, 126, 1143-1170.

Richardson, L. F. (1922). *Weather Prediction by Numerical Process*. Cambridge University Press, 236pp.

Ross, R. J. & Kurihara, Y. (1995). A numerical study on influences of Hurricane Gloria (1985) on the environment. *Mon. Wea. Rev.*, 123, 332-346.

Simmons, A. J. & Hollingsworth A. (2002). Some aspects of the improvement in skill of numerical weather prediction. *Quart. J. Roy. Meteor. Soc.,* 128, 647-677.

Skamarock, W. C.; Klemp, J. B.; Dudhia, J.; Gill, D. O.; Barker, D. M.; Wang, W. & Powers, J. (2005). A Description of the Advanced Research WRF Version 2. *NCAR Technical Note,* TN-468+STR. 88 pp.

Sun, J. & Crook, N. A. (1997). Dynamical and microphysical retrieval from Doppler radar observations using a cloud model and its adjoint. Part I: Model development and simulated data experiments. *J. Atmos. Sci.,* 54, 1642–1661.

Sun, J. & Crook, N. A. (1998). Dynamical and microphysical retrieval from Doppler radar observations using a cloud model and its adjoint. Part II: Retrieval experiments of an observed Florida convective storm. *J. Atmos. Sci.,* 55, 835–852.

Thépaut, J.-N. & Courtier, P. (1991). Four-dimensional data assimilation using the adjoint of a multilevel primitive equation model. *Quart. J. Roy. Meteor. Soc*., 117, 1225–1254.

Ueno, M. (1989). Operational bogussing and numerical prediction of typhoon in JMA. *JMA/NPD Tech. Rep.* 28, 48pp. [Available from Japan Meteorological Agency, Numerical Prediction Division, 1-3-4; Ote-Machi, Chiyodaku, Tokyo, 100, Japan.]

Ueno, M. (1995). A study of the impact of asymmetric components around tropical cyclone center on the accuracy of bogus data and the track forecast. Meteor. *Atmos. Phys*., 56, 125–134.

Whitaker, J. S. & Hamill, T. M. (2001). Ensemble Data Assimilation without perturbed observations. *Mon. Wea. Rev.,* 130, 1913–1924.

White, A. (2000). A view of the equations of meteorological dynamics and various approximations, *Met Office Forecasting Research Scientific Paper,* 58, 88 pp.

Willoughby, H. E. & Black, P. G. (1996). Hurricane Andrew in Florida: Dynamics of a disaster. *Bull. Amer. Meteor. Soc*., 77, 543-549.

Xiao, Q.; Zou, X. & Wang, B. (2000). Initialization and simulation of a landfalling hurricane using a variational bogus data assimilation scheme. *Mon. Wea. Rev*., 128, 2252-2269.

Xiao, Q.; Zou, X.; Pondeca, M.; Shapiro, M. A.; & Velden, C. S. (2002). Impact of GMS-5 and GOES-9 satellite-derived winds on the prediction of a NORPEX extratropical cyclone. *Mon. Wea. Rev*., 130, 507-528.

Xiao, Q.; Kuo, Y.-H.; Sun, J.; Lee, W.-C.; Lim, E.; Guo, Y.-R. & Barker, D. M. (2005). Assimilation of Doppler radar observations with a regional 3D-Var system: Impact of Doppler velocities on forecasts of a heavy rainfall case. *J. Appl. Meteor*, 44, 768-788.

Xiao, Q. & Sun, J. (2007). Multiple-radar data assimilation and short-range quantitative precipitation forecasting of a squall line observed during IHOP_2002. *Mon. Wea. Rev*., 135, 3381-3404.

Xiao, Q.; Kuo, Y.-H.; Zhang, Y.; Barker, D. M. & Won, D.-J. (2006). A tropical cyclone bogus data assimilation scheme in the MM5 3D-Var system and numerical experiments with Typhoon Rusa (2002) near landfall. *J. Met. Soc. Japan*, 84, 671-689.

Xiao, Q.; Kuo, Y.-H.; Sun, J.; Lee, W.-C.; Barker, D. M. & Lim, E. (2007). An approach of radar reflectivity data assimilation and its assessment with the inland QPF of Typhoon Rusa (2002) at landfall. *J. Appl. Meteor. Climat*., 46, 14-22.

Xiao, Q. & coauthors (2008a). Application of an adiabatic WRF adjoint to the investigations of the May 2004 McMurdo Antarctica severe wind event. *Mon. Wea. Rev*., 136, 3696-3713.

Xiao, Q. & coauthors (2008b). Doppler radar data assimilation in KMA's operational forecasting. *Bull. Amer. Meteor. Soc*., 89, 39-43.

Xiao, Q.; Zhang, X.; Davis, C. A.; Tuttle, J. D.; Holland, G. J. & Fitzpatrick, P. J. (2009a). Experiments of hurricane initialization with airborne Doppler radar data for the Advanced-research Hurricane WRF (AHW) model. *Mon. Wea. Rev*., 137, 2758-2777.

Xiao, Q.; Chen, L. & Zhang, X. (2009b). Evaluations of BDA scheme using the Advanced Research WRF (ARW) model. *J. Appl. Meteor. Climat*., 48, 680-689.

Zhang, X.; Xiao, Q. & Fitzpatrick, F. J. (2007). The impact of multi-satellite data on the initialization and simulation of Hurricane Lili's (2002) rapid weakening phase. *Mon. Wea. Rev*., 135, 526-548.

Zou, X. & Xiao, Q. (2000). Studies on the initialization and simulation of a mature hurricane using a variational bogus data assimilation scheme. *J. Atmos. Sci*., 57, 836-860.

Zupanski, M. (2005). Maximum likelihood ensemble filter: theoretical aspects. *Mon. Wea. Rev*., 133, 1710-1726.

Recent Hurricane Research - Climate, Dynamics, and Societal Impacts

Edited by Prof. Anthony Lupo

ISBN 978-953-307-238-8
Hard cover, 616 pages
Publisher InTech
Published online 19, April, 2011
Published in print edition April, 2011

This book represents recent research on tropical cyclones and their impact, and a wide range of topics are covered. An updated global climatology is presented, including the global occurrence of tropical cyclones and the terrestrial factors that may contribute to the variability and long-term trends in their occurrence. Research also examines long term trends in tropical cyclone occurrences and intensity as related to solar activity, while other research discusses the impact climate change may have on these storms. The dynamics and structure of tropical cyclones are studied, with traditional diagnostics employed to examine these as well as more modern approaches in examining their thermodynamics. The book aptly demonstrates how new research into short-range forecasting of tropical cyclone tracks and intensities using satellite information has led to significant improvements. In looking at societal and ecological risks, and damage assessment, authors investigate the use of technology for anticipating, and later evaluating, the amount of damage that is done to human society, watersheds, and forests by land-falling storms. The economic and ecological vulnerability of coastal regions are also studied and are supported by case studies which examine the potential hazards related to the evacuation of populated areas, including medical facilities. These studies provide decision makers with a potential basis for developing improved evacuation techniques.

InTech Europe
University Campus STeP Ri
Slavka Krautzeka 83/A
51000 Rijeka, Croatia
Phone: +385 (51) 770 447
Fax: +385 (51) 686 166

InTech China
Unit 405, Office Block, Hotel Equatorial Shanghai
No.65, Yan An Road (West), Shanghai, 200040, China
中国上海市延安西路65号上海国际贵都大饭店办公楼405单元
Phone: +86-21-62489820
Fax: +86-21-62489821